Drug Design, Development and Therapy

Dovepress
open access to scientific and medical research

Open Access Full Text Article

ORIGINAL RESEARCH

5H-benzo[h]thiazolo[2,3-b]quinazolines ameliorate NDEA-induced hepatocellular carcinogenesis in rats through IL-6 downregulation along with oxidative and metabolic stress reduction

Drug Design, Development and Therapy downloaded from https://www.dovepress.com/
For personal use only.

This article was published in the following Dove Press journal:
Drug Design, Development and Therapy
13 October 2017
Number of times this article has been viewed

Amit K Keshari[1]
Ashok K Singh[1]
Umesh Kumar[2]
Vinit Raj[1]
Amit Rai[1]
Pranesh Kumar[1]
Dinesh Kumar[2]
Biswanath Maity[2]
Sneha Nath[3]
Anand Prakash[3]
Sudipta Saha[1]

[1]Department of Pharmaceutical Sciences, Babasaheb Bhimrao Ambedkar University, [2]Centre of Biomedical Research, SGPGIMS Campus, [3]Department of Biotechnology, Babasaheb Bhimrao Ambedkar University, Lucknow, India

Abstract: 5H-benzo[h]thiazolo[2,3-b]quinazoline scaffold is known to have an antitumor effect on certain types of malignancies; however, its effect on hepatocellular carcinoma (HCC) remains unclear. Previously, we reported *p*-toluenesulfonic acid-promoted syntheses, molecular modeling and in vitro antitumor activity of 5H-benzo[h]thiazolo[2,3-b]quinazoline against human hepatoma (Hep-G2) cells where compounds **4A** and **6A** were found to be potent inhibitors among the series. In continuation to our previous effort to develop novel therapeutic strategies for HCC treatment, here we investigated the in vivo antitumor activity and the mechanism underlying the effects of **4A** and **6A** in N-nitrosodiethylamine (NDEA)-induced HCC using male Wistar rats. NDEA was administered weekly intraperitoneally at a dose of 100 mg/kg for 6 weeks. Various physiological and morphological changes, oxidative parameters, liver marker enzymes and cytokines were assessed to evaluate the antitumor effect of **4A** and **6A**. In addition, proton nuclear magnetic resonance-based serum metabolomics were performed to analyze the effects of **4A** and **6A** against HCC-induced metabolic alterations. Significant tumor incidences with an imbalance in carcinogen metabolizing enzymes and cellular redox status were observed in carcinogenic rats. Tumor inhibitory effects of **4A** and **6A** were noted by histopathology and biochemical profiles in NDEA-induced hepatic cancer. Compounds **4A** and **6A** had a potential role in normalizing the elevated levels of inflammatory mediators such as interleukin-1β (IL-1β), IL-2, IL-6 and IL-10. At molecular level, the real-time quantitative reverse-transcribed polymerase chain reaction analysis revealed that **4A** and **6A** attenuated the *IL-6* gene overexpression in hepatic cancer. Further, orthogonal partial least squares discriminant analysis scores plot demonstrated a significant separation of **4A** and **6A**-treated groups from carcinogen control group. Both the compounds have potential to restore the imbalanced metabolites due to HCC, signifying promising hepatoprotective activities. All these findings suggested that **4A** and **6A** could be potential drug candidates to treat HCC.

Keywords: 5H-benzo[h]thiazolo[2,3-b]quinazoline, N-nitrosodiethylamine, NDEA, hepatocellular carcinoma, HCC, interleukins, ^{1}H-NMR based metabolomics

Introduction

Chronic exposure to chemical carcinogens leads to several biochemical and genetic variations in the cells. N-nitrosodiethylamine (NDEA), a known toxic and environmental hepatic carcinogen, has been used as a tumor inducer in various hepatic cancer models. Also, it has been shown to be mutagenic and genotoxic.[1] Cytochrome P450 enzyme-dependent NDEA metabolism produces reactive oxygen species (ROS) and

Correspondence: Sudipta Saha
Department of Pharmaceutical Sciences, Babasaheb Bhimrao Ambedkar University, Vidya Vihar, Raebareli Road, Lucknow, Uttar Pradesh 226025, India
Tel +91 80 9074 7008
Email sudiptapharm@gmail.com

submit your manuscript | www.dovepress.com
Dovepress
http://dx.doi.org/10.2147/DDDT.S143075

© 2017 Keshari et al. This work is published and licensed by Dove Medical Press Limited. The full terms of this license are available at https://www.dovepress.com/terms.php and incorporate the Creative Commons Attribution – Non Commercial (unported, v3.0) License (http://creativecommons.org/licenses/by-nc/3.0/). By accessing the work you hereby accept the Terms. Non-commercial uses of the work are permitted without any further permission from Dove Medical Press Limited, provided the work is properly attributed. For permission for commercial use of this work, please see paragraphs 4.2 and 5 of our Terms (https://www.dovepress.com/terms.php).

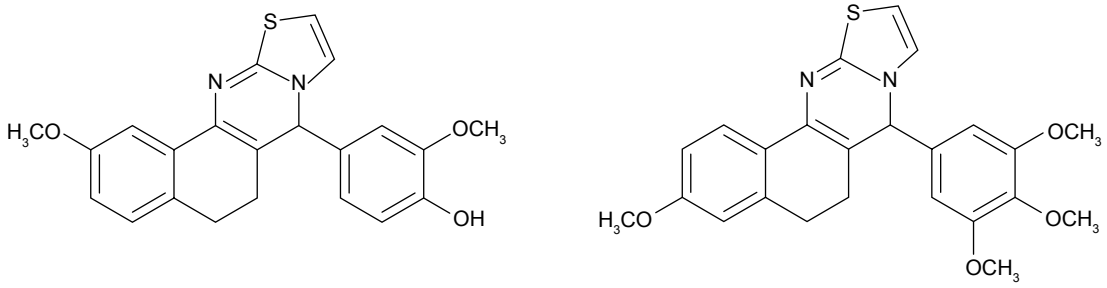

Figure 1 Chemical structures of **4A** (2-methoxy-4-(2-methoxy-6,7-dihydro-5H-benzo[h] thiazolo[2,3-b]quinazolin-7-yl)phenol) and **6A** (3-methoxy-7-(3,4,5-trimethoxyphenyl)-6,7-dihydro-5H-benzo[h]thiazolo[2,3-b]quinazoline).

also other free radicals, which may be responsible for its tumorigenic activity.[2,3] Currently, NDEA-induced hepatocellular carcinoma (HCC) in rats is extensively used as a standard experimental model to investigate the different stages of hepatocarcinoma.[4]

Dysregulated cell proliferation and solid tumor generation are generally encountered in several cancers including HCC. The mechanism of cancer development is mainly due to the activation of oncogenes and inactivation of tumor suppressor genes (TSG).[4,5] HCC is one of the most common malignancies with high prevalence and poor prognosis and the second leading cause of cancer-associated deaths worldwide.[6,7] Its rate of incidence is dramatically increasing in developing countries due to increased underlying hepatic conditions, for instance, alcoholic liver disease, non-alcoholic fatty liver disease and hepatitis B and C infection. The worldwide mortality rate of all other leading cancers (such as lung, breast and prostate cancers) is declining, whereas the death rate of liver cancer is increased by 2.8% in men and 3.4% in women each year.[8,9] Approximately 748,000 new cases (9.2% of all new global cancer cases) of HCC are being diagnosed every year worldwide.[10]

As per reports, chemotherapy with standard cytotoxic agents such as doxorubicin, cisplatin or 5-fluorouracil shows below 10% response rate without a clear benefit in overall survival.[11,12] In addition, these are poorly tolerated in patients as a result of systemic toxicities and their associated adverse effects.[13] In fact, one of the most challenging applications in the emerging field of HCC treatment is to develop new therapeutic strategies for solid tumors with negligible or lesser cytotoxicity to the normal cells.

Functionalized thiazolo[2,3-b]quinazoline scaffolds have long been studied and served as a versatile building blocks in the emerging field of synthetic medicinal chemistry.[14,15] This privileged structural motif is known for its wide range of biological activities[16–19] including anticancer,[20] anti-inflammatory,[21] antituberculosis,[22] anticonvulsant,[23] antimalarial,[24] antihypertensive,[25] antidiabetic,[26] etc.

Previously, we reported *p*-toluenesulfonic acid-promoted syntheses, molecular modeling and in vitro antitumor activity of newly synthesized 5H-benzo[h]thiazolo[2,3-b]quinazolines against human hepatoma (Hep-G2) cells where compounds **4A** and **6A** (Figure 1) were found as potent inhibitors among the series.[27] In continuation to our previous effort to develop novel therapeutic strategies for HCC treatment, we investigated the in vivo antitumor activity involving the role of oxidative stress parameters and inflammatory mediators in NDEA-induced HCC using male albino Wistar rats. The molecular mechanism underlying the antitumor effects of **4A** and **6A** was explored by observing the gene expression levels through real-time quantitative reverse-transcribed polymerase chain reaction (qRT-PCR) analysis. Later, proton nuclear magnetic resonance (^{1}H-NMR)-based serum metabolomics were performed to analyze the effects of **4A** and **6A** against HCC-induced metabolic alterations.

Materials and methods

Materials

NDEA, glutathione (GSH) and 2,4-dinitrophenylhydrazine were acquired from Sigma-Aldrich, St Louis, MO, USA. Alanine aminotransferase (ALT) and aspartate aminotransferase (AST) kits were purchased from the Transasia Biomedicals Pvt. Ltd., Baddi, India. Interleukin (IL)-2 and IL-6 were commercially procured from Sigma-Aldrich and IL-1β and IL-10 from Genetex Biotech Asia Pvt. Ltd, New Delhi, India. All the chemicals and solvents were of analytical grades with 99% purity, and in-house distilled water was used throughout the experiment. Test compounds **4A** and **6A** were synthesized previously by our research group.[27]

Experimental animals

Healthy male Wistar albino rats, weighing 80–120 g, were obtained from central animal house facility of SD College of Pharmacy & Vocational Studies, Muzaffarnagar, India in association with Babasaheb Bhimrao Ambedkar University,

Lucknow, India, and were housed in polypropylene cages with rice husks for bedding. Animal welfare protocol and experiments were performed as per CPCSEA guidelines for laboratory animals and ethics, Department of Animal Welfare, Government of India. The Institutional Animal Ethical Committee of SD College of Pharmacy & Vocational Studies approved this study (approval no SDCOP&VS/AH/CPCSEA/01/0038/R1). Animals were acclimatized under standard laboratory conditions (at 25°C±5°C; relative humidity of 44%–56%; 12 h light:dark cycle) with free access of standard rat chow and water ad libitum.

Acute toxicity study

Acute oral toxicity study of both **4A** and **6A** was performed as per revised Organization for Economic Cooperation and Development guidelines 423. Both **4A** and **6A** were dissolved in 0.25% carboxymethyl cellulose (CMC) and administered orally at the dose of 5 and 10 mg/kg body weight to albino Wistar rats for 15 days (n=10) and the animals were observed every day for any toxic manifestations.

Experimental design

All the experimental Wistar rats were randomly distributed into 5 groups of 8 animals each (n=8) and the groups were classified as group I (normal control): 0.25% CMC (2 mL/kg); group II (carcinogen control): NDEA (100 mg/kg, i.p. every week for 6 weeks);[28–30] group III (positive control): NDEA+5-FU (10 mg/kg, i.p. for 15 days after the dose of NDEA administration); group IV (**4A**): NDEA+**4A** (10 mg/kg, orally for 15 days after the dose of NDEA administration) and group V (**6A**): NDEA+**6A** (10 mg/kg, orally for 15 days after the dose of NDEA administration).

The abovementioned protocol to induce HCC was adopted from various literatures.[31,32] After adaptive inhabitation to experimental conditions for initial 1 week, all experimental animals of group II to V were administrated with NDEA. After the dose of NDEA administration for 6 weeks, 5-FU, **4A** and **6A** were given for 15 days as a curative agent against liver injury, mentioned in groups III, IV and V respectively. At the end of experimental period, animals were sacrificed by cervical decapitation and livers were excised immediately, rinsed in ice-cold saline and stored at −80°C for further histological studies and molecular level investigations. The serum was also collected, processed and stored for further biochemical analysis.

Estimation of various physiological parameters

To estimate the body weight variation, rats were weighed at the initial and final days of experiment and % weight gain calculated to observe the cytotoxic effects between treated and untreated group. Liver weight, number and percentage incidence of carcinogenic nodules of liver were calculated.

Estimation of serum enzyme levels and biochemical examination in liver

Serum enzymes, including AST, ALT, lactate dehydrogenase (LDH) and creatine phosphokinase (CK) were measured using commercially available kit. The oxidative stress parameters like catalase (CAT),[33] protein carbonyl (PC),[34] superoxide dismutase (SOD),[35] GSH[36] and thiobarbituric acid reactive substances (TBARS)[33] were also estimated in liver tissue in the similar way as described previously. The total protein concentration of each sample was measured using the Bradford reagent, and bovine serum albumin (BSA) was used as a standard.

Estimation of catabolic byproducts in hepatic tissue: bilirubin and biliverdin

Conjugated bilirubin and biliverdin in liver were measured as per the previously explained protocols.[37]

Estimation of cytokines in hepatic tissue

Elevated levels of IL-1β, IL-2, IL-6 and IL-10 inflammatory mediators were assayed as per the instructions provided by the manufacturers. Rat IL-1β, IL-2, IL-6 and IL-10 enzyme-linked immunosorbent assay (ELISA) kits were based on standard sandwich ELISA technology.

Histopathological studies and scanning electron microscopy of hepatic tissue

The procedures adopted for histopathology and scanning electron microscopy (SEM) were described previously.[38]

qRT-PCR analysis

To determine the expression of mRNA for the different genes, 10 mg of tissue samples of each group was taken in a tube and total RNA was extracted using TriZol reagent, and RNeasy mini kit was employed to purify the RNA. cDNA reactions were prepared utilizing GeneSure first-strand cDNA synthesis kit (Genetix Biotech Asia Pvt. Ltd., New Delhi, India) for quantitative PCR. Finally, real-time PCR was carried out in Agilent Stratagene Mx3000P series (Applied Biosystems, Waltham, MA, USA) using Sybr@ green PCR master mix. The mRNA was normalized with housekeeping control β-actin. ΔCt values were normalized with untreated control samples for all compounds ($\Delta Ct = Ct_{\text{gene of interest}} - Ct_{\text{housekeeping gene}}$). Relative changes in the expression level

of one specific gene were calculated in terms of 2-ΔΔCt ($\Delta\Delta Ct = \Delta Ct_{test} - \Delta Ct_{control}$).[34]

The primer sequences were as follows: GAPDH, 5′-TGATGGGTTTCCCATTGATGA-3′ (forward) and 5′-TGATTCTACCCACGGCAAGTT-3′ (reverse);[39] IL-6, 5′-TCAATGAGGAGACTTGCCTG-3′ (forward), 5′-GATGAGTTGTCATGTCCTGC-3′ (reverse).[40]

^{1}H-NMR-based serum metabolic profiling

Sample preparation and NMR instrumentation

An aliquot of serum (250 µL) from each sample and 250 µL of 0.9% of an aqueous saline solution (50 mM concentration, pH 7.4 in D_2O) were taken in 2 mL Eppendorf tube and centrifuged at 10,000 rpm for 5 min. The supernatant was transferred to a 5 mm NMR tube (Wilmad Lab Glass, Vineland, NJ, USA) for data recording. As external standard, 0.1% (v/v) TSP (sodium salt of 3-trimethylsilyl-(2,2,3,3-d4)-propionic acid) was mixed in NMR tube.

The NMR spectra of prepared samples were generated at 298 K on a Bruker Biospin Avance-III 800 MHz NMR spectrometer, operating at proton frequency of 800.21 MHz. The spectrometer is equipped with CryoProbe with maximum gradient strength output of 53 G/cm. 1D ^{1}H-NMR spectra were recorded using the Carr–Purcell–Meiboom–Gill (CPMG) pulse sequence in Topspin-2.1 (Bruker NMR data Processing Software) with pre-saturation of the water peak via irradiating it perpetually during the recycle delay of 5 sec. Each CPMG spectrum consisted of accumulation of 128 scans and lasted for approximately 15 min. A total spin–spin relaxation time of 60 ms (n=300 and 2τ=200 δs) with a line-broadening factor of 0.3 Hz was applied to remove broad signals from triglycerides, proteins, cholesterols and phospholipids. Diffusion time of 120 ms was used to enervate the signals of low molecular weight compounds without affecting the lipid signals. All the acquired NMR spectra were processed using Topspin-2.1 (Bruker NMR data Processing Software) and standard Fourier transformation (FT) procedure for phase and baseline correction. Prior to FT, each free induction decays were zero-filled to 4096 data points and a sine-bell apodization function/tapering function was applied. After FT, the chemical shifts were referenced internally to methyl doublet of L-lactate (at δ=1.33 ppm). All the recorded spectra were visually analyzed for their acceptability and subjected to multivariate statistical analysis to identify the altered metabolic pattern.

Spectral assignment

To identify the distinct allocation of various peaks in the CPMG ^{1}H-NMR spectra, two-dimensional NMR spectra were recorded for selected samples including ^{1}H-^{1}H total correlation spectroscopy and ^{1}H-^{13}C heteronuclear single quantum correlation. The chemical shifts were identified and assigned at a good extent by comparing them with the chemical shifts available with the software Chenomx 8.1 (Chenomx Inc., Edmonton, AB, Canada). The remaining peaks in the CPMG ^{1}H-NMR spectra were allocated using the previously existing databases available as HMDB (The Human Metabolome Database) and other literature reports.[41–43]

Multivariate data analysis

All the acquired NMR spectra were corrected manually for phase and baseline aberration in Topspin 2.1 (Bruker NMR data Processing Software). The CPMG (δ 0.5−8.5 ppm) spectra were then binned into 0.01 ppm wide integrated spectral buckets with the help of AMIX package (Version 3.8.7, Bruker BioSpin). The regions containing the resonance from residual water (δ 4.7–5.1 ppm) were excluded to avoid the effects of imperfect water suppression. The binned data were then obtained from AMIX after mean centering and normalization, which was executed by dividing each data point by the sum of all data points present in the sample, to compensate for the differences in concentration of metabolites among individual serum samples.

The data were scaled up using unit variance where identical weight was given to all variables. The resulting data matrices were exported into Microsoft Office Excel 2010 and used for multivariate analysis via open access web-based metabolomic data processing tool, named MetaboAnalyst 3.0 (http://www.metaboanalyst.ca/) and Unscrambler X Software (Version 10.3, CAMO USA, Norway). Principal component analysis (PCA) was first performed on both the CMPG and sets to identify the outliers. To further demonstrate the separation between samples belonging to different groups, supervised partial least squares discriminant analysis (PLS-DA) was performed to identify the metabolites significantly contributing to group differentiation. Model quality was assessed with R^2, indicating the validity of models against over fitting, and Q^2, indicating the predictive ability. Potential metabolites markers were extracted from PLS-DA loading plots and the scores of variable importance in projection (VIP). The statistical significance of these metabolites was calculated by Student's *t*-test (*p*-value less than 0.05).

Statistical data analysis

Statistical data analysis was performed using Graph Pad Prism 5.0 (San Diego, CA, USA). All results were expressed

as mean ± standard deviation. The data were analyzed by one-way analysis of variance followed by Bonferroni multiple comparison test. Statistical significance differences were considered with respect to carcinogen control (*$p<0.001$, **$p<0.01$, ***$p<0.05$).

Results

Acute oral toxicity study

No mortality and behavioral changes were observed up to 15 days. Various biological parameters such as AST and ALT in plasma; bilirubin and biliverdin in serum; and various biochemical parameters (SOD, CAT, PC, GSH, TBARS) in liver were measured during this study. We found that there were no significant changes in any of these parameters following **4A** and **6A** treatments (dose 5 and 10 mg/kg) as compared to normal control (data not shown). Results obtained from acute oral toxicity studies implied that both compounds were safe up to 10 mg/kg body weight dose in albino Wistar rats. Therefore, we decided to perform anti-HCC activity at a dose of 10 mg/kg body weight.

Estimation of physiological and biochemical parameters in liver tissue and various enzyme levels in serum

In the present study, we initially analyzed the defensive efficiency of **4A**, **6A** and 5-FU through various physiological parameters like body weight, liver weight, number and percentage incidence of carcinogenic nodules in liver of experimental groups of animals, respectively. The body weight and liver weight variation were more prominent in NDEA-administered (group II) rats as compared to the normal control (group I) rats; conversely, treatment with **4A** and **6A** normalized the impact to a certain extent (Table 1). Similar observations were noted for carcinogenic nodule no per animal and % incidence of carcinogenic nodules in liver. The test compounds and 5-FU significantly ($p<0.05$) lowered the NDEA-induced carcinogenic nodules and % incidence as compared to group II (Table 2). As already mentioned, the administration of **4A**, **6A** and 5-FU normalized these parameters to a certain level. Interestingly, the impact of **4A** was nearly similar to the standard chemotherapeutic drug, 5-FU.

Table 3 depicts the reduction of oxidative stress markers (SOD, CAT, GSH, TBARS and PC) after drug treatment, and the status of hepatic antioxidant potential was investigated in NDEA-exposed groups to explore the functional correlation between oxidative stress and cancer progression. We observed that the GSH concentration was greatly reduced in NDEA-exposed rats, whereas treatment with 5-FU, **4A** and **6A** efficiently increased the GSH content towards normal (Table 3). Besides this, we noticed that the levels of SOD and CAT enzymes were reduced up to 50% and 70%, respectively, after NDEA exposure, while a minor reduction in these enzymatic activities was observed in **4A** and **6A**-treated groups with respect to control. By contrast, a significant increase in MDA and PC formation was seen in HCC rats but these formations were most efficiently regained after 5-FU, **4A** and **6A** treatment (Table 3).

Figure 2 indicates the level of serum liver marker enzymes such as AST, ALT, LDH and CK in normal control and experimental animals. NDEA-induced carcinogenic control (group II) animals exhibited almost twofold increase ($p<0.01$) in the levels of these enzymes when compared to normal control (group I). However, treatment with test compounds **4A** and **6A** showed their ability in the maintenance of these enzymatic activities.

Estimation of catabolic byproducts (bilirubin and biliverdin) in hepatic tissue

4A and **6A**-treated (groups IV and V, respectively) rats reflect significant ($p<0.01$) normalization of the catabolic pigments in liver tissues as compared to carcinogenic control group (group II) which, in turn, exhibited almost twofold significant ($p<0.001$) elevation as compared to normal control, indicating the toxic nature of NDEA (Figure 3).

Table 1 Effects of **4A** and **6A** on body weight and liver weight in hepatocellular carcinoma after oral administration of a dose of 10 mg/kg for 15 days

Groups	Initial body weight (g)	Final body weight (g)	Weight gain (g)	Percentage growth	Liver weight (g)
NC	97.33±10.08	144.50±2.46	47.17±6.72	33	7.17±0.20
CC	105.67±13.74	116.83±12.09	11.17±1.47	10	10.69±0.82
PC	101.17±10.06	130.50±5.04*	29.33±3.02*	22	7.58±0.31*
4A	100.33±6.95	131.39±4.11*	31.33±1.92*	24	8.00±0.16**
6A	102.17±4.81	130.61±6.18*	24.83±1.94*	19	8.83±0.11**

Notes: Data represented as mean ± SD (n=8). Statistically significant differences were observed between carcinogen control and test groups (one-way ANOVA followed by Bonferroni multiple comparison test [*$p<0.001$, **$p<0.01$]).
Abbreviations: ANOVA, analysis of variance; CC, carcinogen control; NC, normal control; PC, positive control.

Table 2 Effects of **4A** and **6A** on the incidence of nodules after oral administration of 10 mg/kg for 15 days

Groups	No of animal bearing nodules/total animals	% incidence of nodules[a]	Total no of nodules	No of nodules per animal[b]
NC	0/6	0	0	0
CC	6/6	100	41	7
PC	3/6	50	7	1
4A	4/6	66.67	11	2
6A	5/6	83.33	22	4

Notes: [a](Number of nodules bearing rats/total number of rats in each group) ×100. [b](Total number of tumor/number of tumor bearing rats in each group).
Abbreviations: CC, carcinogen control; NC, normal control; PC, positive control.

Effect of 4A and 6A on IL-1β, IL-2, IL-6 and IL-10 levels

To further characterize the effects of **4A** and **6A** in the inflammatory events, we investigated the tissue concentration of the specific inflammatory cytokines viz IL-1β, IL-2, IL-6 and IL-10 by ELISA. The concentration of these cytokines in rat hepatic tissue was increased significantly by twofold to threefold after NDEA treatment as compared to normal control. Both the test compounds and 5-FU significantly suppressed the abnormally high concentration of these mediators in tumors tissues. Treatment with **4A** and **6A** (10 mg/kg) attenuated the increased levels of IL-1β, IL-2, IL-6 and IL-10 with pronounced effect on IL-6. Compound **4A**-treated group showed inhibition of IL-6 level as well as other cytokines level ($p<0.001$), more similar to 5-FU (Table 4).

Impact of the test compound on IL-6 gene expression

Our findings suggest that NDEA-alone administration dramatically elevated the IL-6 levels compared to untreated group (group I). However, 5-FU, **4A** and **6A** treatment significantly normalized the elevated levels of IL-6. The efficacy of **4A** and **6A** at 10 mg/kg dose was nearly equivalent to commercially available chemotherapeutic drug 5-FU, and **4A** was found to be potent than **6A** (Figure 4).

Morphology, histopathology and SEM analysis

Morphological changes were observed using intact liver of various groups. There was a clear visual difference in the numbers of carcinogenic nodules between **4A**, **6A** and NDEA-administered groups. Histological changes of hepatic tissue were observed in various treated groups compared to normal control. Hepatic tissue analysis exhibited loss of architecture and the presence of enlarged hepatocytes in carcinogen control than normal control. The NDEA-administered groups also exhibited irregular sinusoids and degenerated tumor cells. The rats treated with **4A** and **6A** (10 mg/kg) showed cells with architecture more or less similar to normal control (Figure 5) and the effects were similar to 5-FU. SEM analysis also followed the similar patterns where loss of architecture and degenerated tumor cells were less prominent in **4A**, **6A** and 5-FU treated rats as compared to NDEA-exposed rats (Figure 5).

^{1}H-NMR-based metabolomics

Metabolic effects of **4A** and **6A** in NDEA-induced HCC rats

Acquired NMR data from the serum samples of all the groups were analyzed using SIMCA-P software, version 11.0 (Umetrics AB, Umea, Sweden) where chemometric

Table 3 Effects of **4A** and **6A** on oxidative stress parameters in hepatocellular carcinoma after oral administration of a dose of 10 mg/kg for 15 days

Groups	SOD (U/mg of protein)	CAT (mM H_2O_2 decomposed/min/mg of protein)	GSH (μM/mg of protein)	TBARS (nM of MDA/mg of protein)	PC (μM/mg of protein)
NC	0.34±0.02	6.07±0.55	16.48±0.53	0.31±0.04	0.12±0.01
CC	0.15±0.01	1.78±0.25	8.92±0.67	0.53±0.03	1.13±0.04
PC	0.30±0.04*	5.41±0.68*	13.04±0.49*	0.33±0.04**	0.15±0.02*
4A	0.27±0.03*	3.70±0.31*	11.06±0.31*	0.34±0.01**	0.16±0.01*
6A	0.20±0.02**	2.67±0.24**	9.98±0.38**	0.36±0.02**	0.28±0.02**

Notes: Data represented as mean ± SD (n=8). Statistically significant differences were observed between carcinogen control and test groups (one-way ANOVA followed by Bonferroni multiple comparison test [*$p<0.001$, **$p<0.01$]).
Abbreviations: ANOVA, analysis of variance; CAT, catalase; CC, carcinogen control; GSH, glutathione; NC, normal control; PC, positive control; SOD, superoxide dismutase; TBARS, thiobarbituric acid reactive substances.

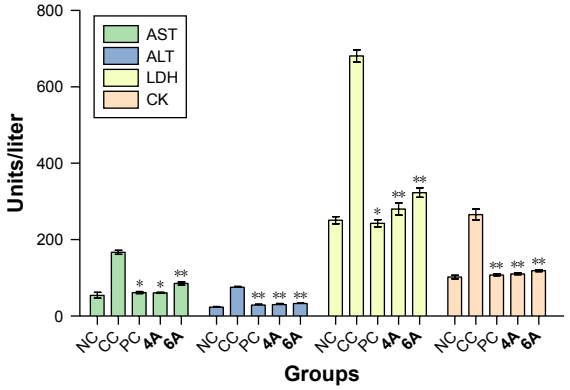

Figure 2 Effects of **4A** and **6A** on enzyme levels in serum after 10 mg/kg dose administration for 15 days.
Notes: Data represented as mean ± SD (n=8). Statistically significant differences were observed between carcinogen control and test groups (one-way ANOVA followed by Bonferroni multiple comparison test [*$p<0.001$, **$p<0.01$]).
Abbreviations: ALT, alanine aminotransferase; ANOVA, analysis of variance; AST, aspartate aminotransferase; CC, carcinogen control; CK, creatine phosphokinase; LDH, lactate dehydrogenase; NC, normal control; PC, positive control.

methods including PCA and orthogonal partial least squares discriminant analysis (OPLS-DA) were performed to examine the metabolic alterations in an unsupervised and supervised manner, respectively. PCA model was applied to authenticate the analytical quality system performance to discern outliers. OPLS-DA model was useful to obtain a summary of set of samples and to discriminate the variables that are responsible for variation among all the groups. The OPLS-DA model was optimized through two variables, ie, Q^2 and R^2Y. Score plots obtained from 1D ^{1}H CPMG NMR spectra (Figure S1) (from OPLS-DA and S plots) exhibited reasonable separation among all groups (Figures 6 and 7).

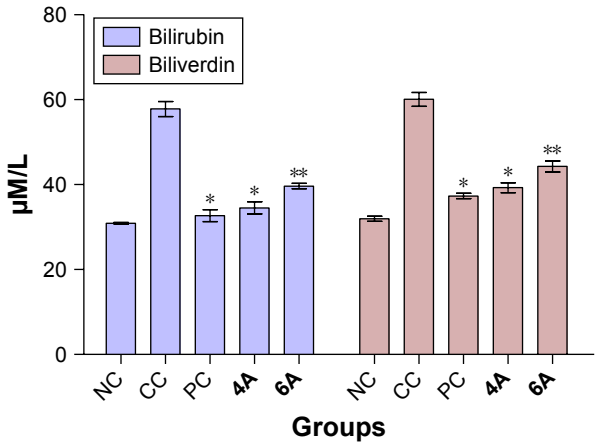

Figure 3 Effects of **4A** and **6A** on catabolic byproduct (bilirubin and biliverdin) after 10 mg/kg dose administration for 15 days.
Notes: Data represented as mean ± SD (n=8). Statistically significant differences were observed between carcinogen control and test groups (one-way ANOVA followed by Bonferroni multiple comparison test [*$p<0.001$, **$p<0.01$]).
Abbreviations: ANOVA, analysis of variance; CC, carcinogen control; NC, normal control; PC, positive control.

The various metabolites were carefully chosen when the statistically major threshold of VIP values achieved from the OPLS-DA model was greater than 1.0. Meanwhile, two-tailed Student's *t*-test *p*-value less than 0.05 ($p<0.05$) was considered statistically significant. Log2 fold change was employed to demonstrate how these selected differential metabolites varied among all the groups of animals. The datasets of these differentially expressed metabolites (log2-scaled) were introduced into MetaboloAnalyst 3.0 for the generation of heat map and multivariate statistics. The areas under the receiver operating characteristic curves were constructed to evaluate the effectiveness of potential biomarkers. In the MetaboAnalyst analysis, the results were considered statistically significant when *p*-value was less than 0.05 (Figure 8).

Metabolic changes during carcinogenic condition with treatments

On the basis of PLS-DA data, both the combined and pairwise analysis revealed R^2=0.70, $Q^2Y \geq 0.90$, indicating the significant metabolic changes in NDEA, **4A** and **6A**-treated groups. The key observation of serum metabolic alterations between the untreated and NDEA-exposed groups together with their chemical shifts (δ) values, VIP score and *p*-value are illustrated in Figures 6 and 7. There were significant elevated levels of lactate, high density lipoprotein, low density lipoprotein, very-low density lipoprotein, tryptophan, tyrosine, creatinine and arginine and decreased levels of glucose, maltose, betaine, leucine, glycerate, glycerol, valine and carnosine in NDEA-treated group. Representative box-cum-whisker plots also supported the significant alterations in the abovementioned metabolite profile (Figure 8). All these metabolites were successfully retrieved after the administration of **4A** and **6A**, particularly at 10 mg/kg dose.

Discussion

Liver is a vital organ, playing an imperative role in various physiological and defensive mechanisms and regulating intermediary metabolism in the body.[44] According to literatures, chemotherapy against HCC has no survival benefits for patients. The clinical outcome of HCC treatment remains limited and unsatisfactory due to systemic toxicities and other side effects.[13,45] Considering these consequences, chemotherapeutic agents may be used in lower dose as well as higher dose, but the higher dosages provide better efficacy profile while the lower dosages give better safety profile. Therefore, these are never-ending balancing acts.[12,46] It is, therefore, urgent to develop probable therapeutic agents for

Table 4 Effects of **4A** and **6A** on IL-2, IL-6, IL-10 and IL-1β in hepatic carcinogenic tissue after oral administration of a dose of 10 mg/kg for 15 days

Groups	IL-2 (pg/mL)	IL-6 (pg/mL)	IL-10 (pg/mL)	IL-1β (pg/mL)
NC	134.03±10.08	39.23±2.46	58.13±6.72	42.50±4.19
CC	330.60±13.74	124.18±12.09	113.31±8.47	110.22±8.49
PC	160.19±10.06*	57.06±5.04*	66.33±6.02*	57.53±5.86*
4A	192.73±6.95*	62.10±4.11*	70.15±10.12*	70.90±10.68**
6A	269.00±4.81**	73.88±6.18**	80.79±1.94**	84.34±2.03**

Notes: Data represented as mean ± SD (n=8). Statistically significant differences were observed between carcinogen control and test groups (one-way ANOVA followed by Bonferroni multiple comparison test [*$p<0.001$, **$p<0.01$]).
Abbreviations: ANOVA, analysis of variance; CC, carcinogen control; IL, interleukin; NC, normal control; PC, positive control.

better efficacy as well as safety profile to sustain the clinical benefits in cancerous patients.

Our research group recently synthesised compounds **4A** and **6A**, which displayed excellent antiproliferative activity on Hep-G2 cells with GI_{50} <10 µg/mL. In silico studies revealed that **4A** and **6A** have impressive binding energy with crucial hydrogen and π–bonds to various HCC biomarkers, ie, IL-2, IL-6, caspase-3 and caspase-8.[27] The present investigation was carried out to evaluate the ameliorative effects of NDEA-induced hepatocellular carcinogenesis in albino Wistar rats by 5H-benzo[h]thiazolo[2,3-b] quinazolines and the role of specific cytokines and oxidative and metabolic stress manifestations during cancer progression. Overall, these findings for the first time clearly suggested the hepatoprotective effect of **4A** and **6A** against NDEA-induced HCC and its ability to bind with important markers more significantly.

On contrary, NDEA-exposed groups showed a decrease in body weight, an increase in liver weight, and a higher number of carcinogenic nodules, which indicates critical HCC condition in rats. However, chemo-drug treatment with **4A**, **6A** and 5-FU significantly regained the various biochemical parameters near to normal. Exposure of animals to **4A**, **6A** and 5-FU after NDEA administration significantly normalized the reduced weight, increased % incidence of carcinogenic nodules, and enhanced the protective action of **4A** and **6A** against carcinogen-induced metabolic alterations in hepatic cells.

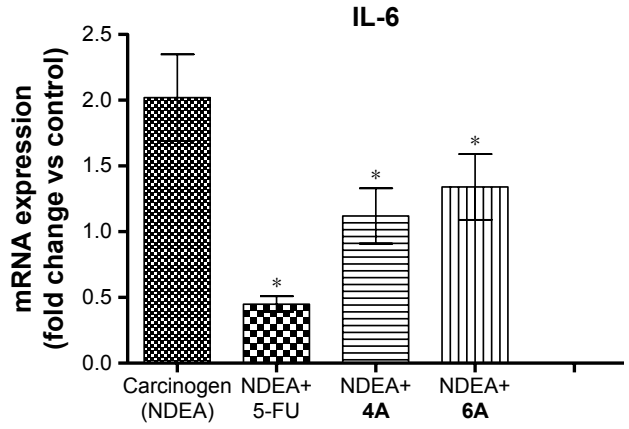

Figure 4 Gene expression levels of pro-inflammatory cytokine IL-6 after **4A** and **6A** administration in NDEA-treated rats.
Notes: Data represented as mean ± SD (n=8). Statistically significant differences were observed between carcinogen control and test groups (paired *t*-test, [*$p<0.001$]).
Abbreviations: IL, interleukin; NDEA, N-nitrosodiethylamine.

Further, oxidative stress-associated biochemical processes diminished the GSH, SOD and CAT levels and conversely the formation of MDA and PC was induced in carcinogen-injected rats. Hence, alterations of these parameters confirmed the onset of hepatic oxidative stress and correlation of transformed cells during cancerous conditions. The formation of excess ROS occurs during the various stages of metabolic biotransformation of NDEA exposure and leads to carcinogenesis by upregulation of several biochemical, intracellular signaling pathways, and gene expression.[47] GSH is a free radical scavenger and SOD, CAT are antioxidant enzymes which inactivate hydrogen peroxide and dismutase superoxides, respectively.[48] Previously, it was reported that there was a decrease in the activities of enzymatic antioxidants during HCC conditions.[49] Cancerous cells have been reported to sequester vital antioxidants from the systemic circulation to achieve the demands of developing solid tumors.[50] Treatment with **4A** and **6A** revealed preventive action to retrieve the levels of GSH, SOD and CAT near to normal and enhanced the anti-oxidative physiological processes. The levels of MDA and PC were attenuated significantly in drug treatment groups as compared to NDEA-exposed HCC rats. Bilirubin and biliverdin are the catabolic byproducts of RBCs, and the elevated levels of these biomarkers indicate hepatic disease state. During this study, it was observed that the levels of bilirubin and biliverdin were elevated in carcinogen-exposed group, whereas **4A** and **6A** treatment significantly attenuated the levels of these two specific markers.[37]

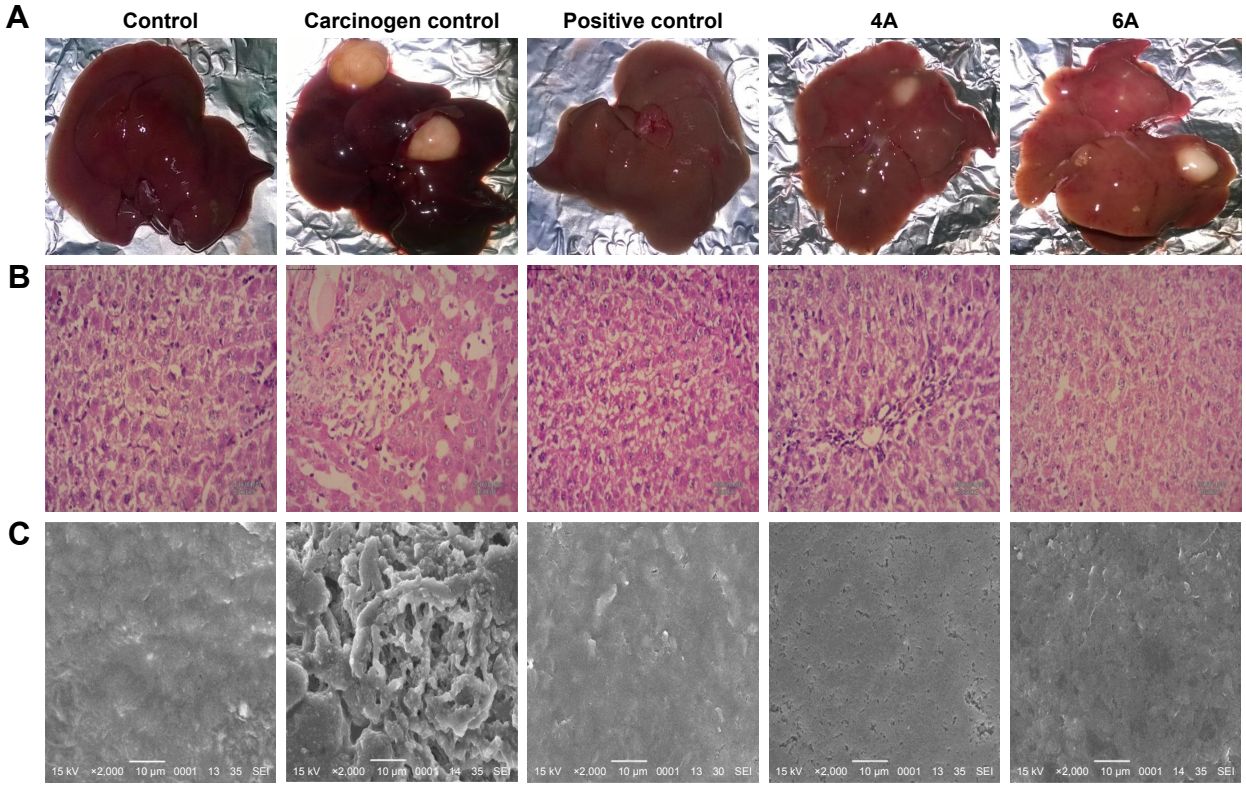

Figure 5 The hepatic pathological changes in NDEA-induced rats.
Notes: Carcinogenic nodules were prominent in the NDEA group, which were absent or reduced significantly after 5-FU, **4A**, and **6A** administration. (**A**) Intact liver, (**B**) histopathological changes (40×, scale bar 50 μm), (**C**) scanning electron microscopic photomicrographs of the liver tissues (2,000×).
Abbreviation: NDEA, N-nitrosodiethylamine.

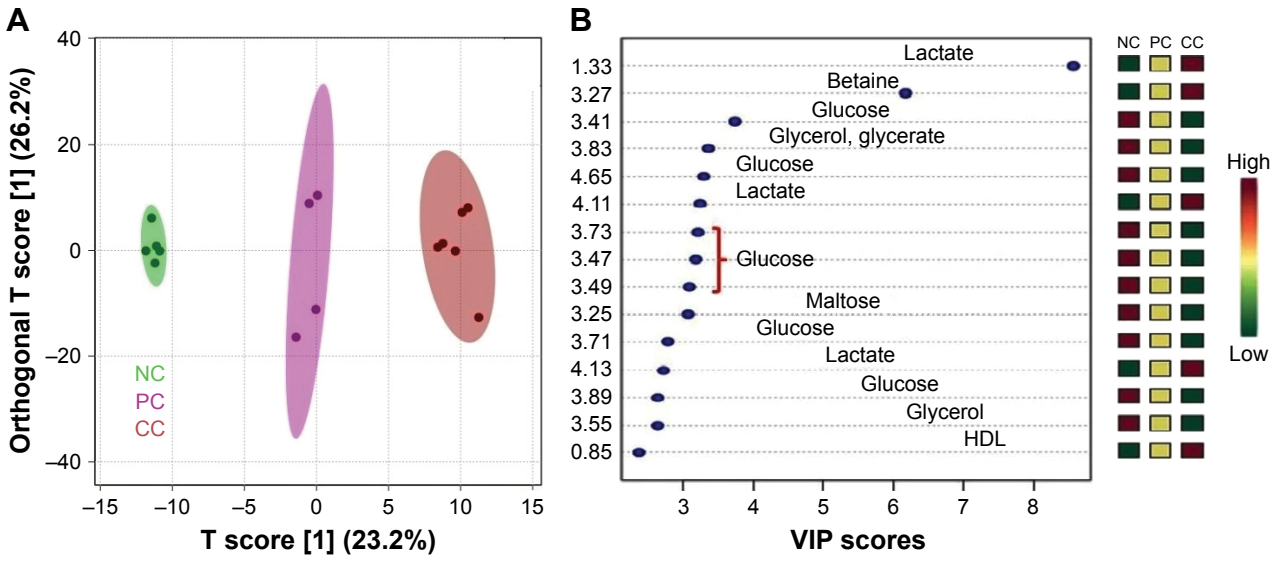

Figure 6 The combined and pairwise OPLS-DA analysis.
Notes: (**A**) 2D OPLS-DA analysis of 1D ^{1}H CPMG NMR spectra score plot derived from combined analysis comprising all the groups: NC, CC, PC, 5-FU, 10 mg/kg (i.p.), pairwise analysis. (**B**) The potential discriminatory metabolite entities identified from VIP scores derived from PLS-DA modeling of complete data matrix and resulting VIP scores for top 20 metabolite entities are shown in increasing order of VIP score values to highlight their discriminatory potential.
Abbreviations: ^{1}H CPMG NMR, proton Carr–Purcell–Meiboom–Gill nuclear magnetic resonance; CC, carcinogen control; NC, normal control; OPLS-DA, orthogonal partial least squares discriminant analysis; PC, positive control; PLS-DA, partial least squares discriminant analysis; VIP, variable importance in projection.

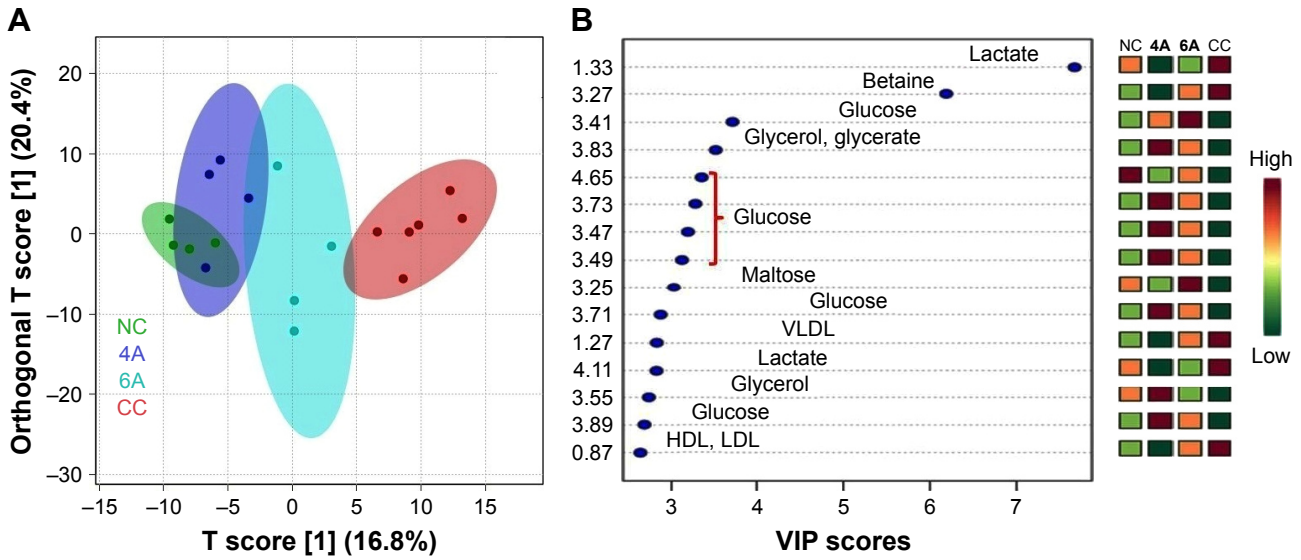

Figure 7 The combined and pairwise OPLS-DA analysis.
Notes: (**A**) 2D OPLS-DA analysis of 1D ^{1}H CPMG NMR spectra score plot derived from combined analysis comprising all the groups: NC, CC, **4A**, and **6A** =10 mg/kg. (**B**) Pairwise analysis. The potential discriminatory metabolite entities identified from VIP scores derived from PLS-DA modeling of complete data matrix and resulting VIP scores for top 20 metabolite entities are shown in increasing order of VIP score values to highlight their discriminatory potential.
Abbreviations: ^{1}H CPMG NMR, proton Carr–Purcell–Meiboom–Gill nuclear magnetic resonance; CC, carcinogen control; NC, normal control; OPLS-DA, orthogonal partial least squares discriminant analysis; PLS-DA, partial least squares discriminant analysis; VIP, variable importance in projection.

Moreover, various enzymes, such as ALT, AST, LDH and CK are notably increased in human serum with liver metastases of HCC.[51] Similar observations were noted in NDEA-exposed rats and the levels were brought down to normalcy with 5-FU, **4A** and **6A** drug treatments; predominantly, the impact of **4A** is comparable to standard 5-FU.

In addition, intact liver architecture, histopathology and SEM analysis were assessed to analyze the morphological changes associated with NDEA administration and drug treatment. Both histology and SEM analyses revealed that degenerated tumor cells, loss of architecture and tumoral vacuoles were formed in NDEA-induced rats as previously reported.[9] The histological investigation of the rats treated with **4A**, **6A** and 5-FU showed cells with architecture more or less similar to control (group I), representing the hepatoprotective activity of the compounds in cancerous condition. In the SEM analysis, we also observed degenerated necrotic tissues in carcinogen-exposed rats, which were regularized to a great extent in **4A** and **6A** treatment groups.

The serum cytokines are key mediators for several pathological and physiological modulations involving inflammation and cancer progression. Further, recent studies indicate that expression of inflammatory mediators like IL-1β, IL-2, IL-6 and IL-10 is involved in initiation and progression of HCC conditions.[52] As per several reports, the regulation of expression and secretion of various cytokines and their receptors have been already described in patients with severe liver conditions.[53,54] For example, circulating blood IL-1β, IL-2, IL-6 and IL-10 concentrations were increased in patients with hepatic cancers.[52–55]

In consequence, with this information related to potential biomarkers, we wanted to know whether **4A** and **6A** may be active against these HCC specific inflammatory cytokines. This observation was further proved by various ELISA assays where all these inflammatory cytokines were elevated in NDEA-exposed rats. In addition, the levels of cytokines were regularized after treatment with **4A**, **6A** and 5-FU, indicating that both the test compounds exhibited anti-HCC property via inhibition of IL-1β, IL-2, IL-6 and IL-10 overexpression at cancer sites. Both the test compounds manifested potential inhibition with IL-6 rather than with IL-1β, IL-2 and IL-10. Similar pattern was also observed in quantitative RT-PCR analysis. The level of *IL-6* gene expression was spectacularly decreased in NDEA-exposed rats (group II) and returned to normal level with **4A**, **6A** and 5-FU treatments, which strongly supported potent anti-HCC activity of **4A**. IL-6 is a pleiotropic four-helical cytokine that modulates inflammation-associated cancers by activating the phosphorylation of STAT3 to promote tumor initiation, invasion and metastasis.[56,57] However, increased levels of IL-6 have been reported to be related to HCC prognosis with elevated cancer risk.[58]

^{1}H-NMR-based metabolomics were further implemented to evaluate whether **4A** and **6A** have ability to restore the

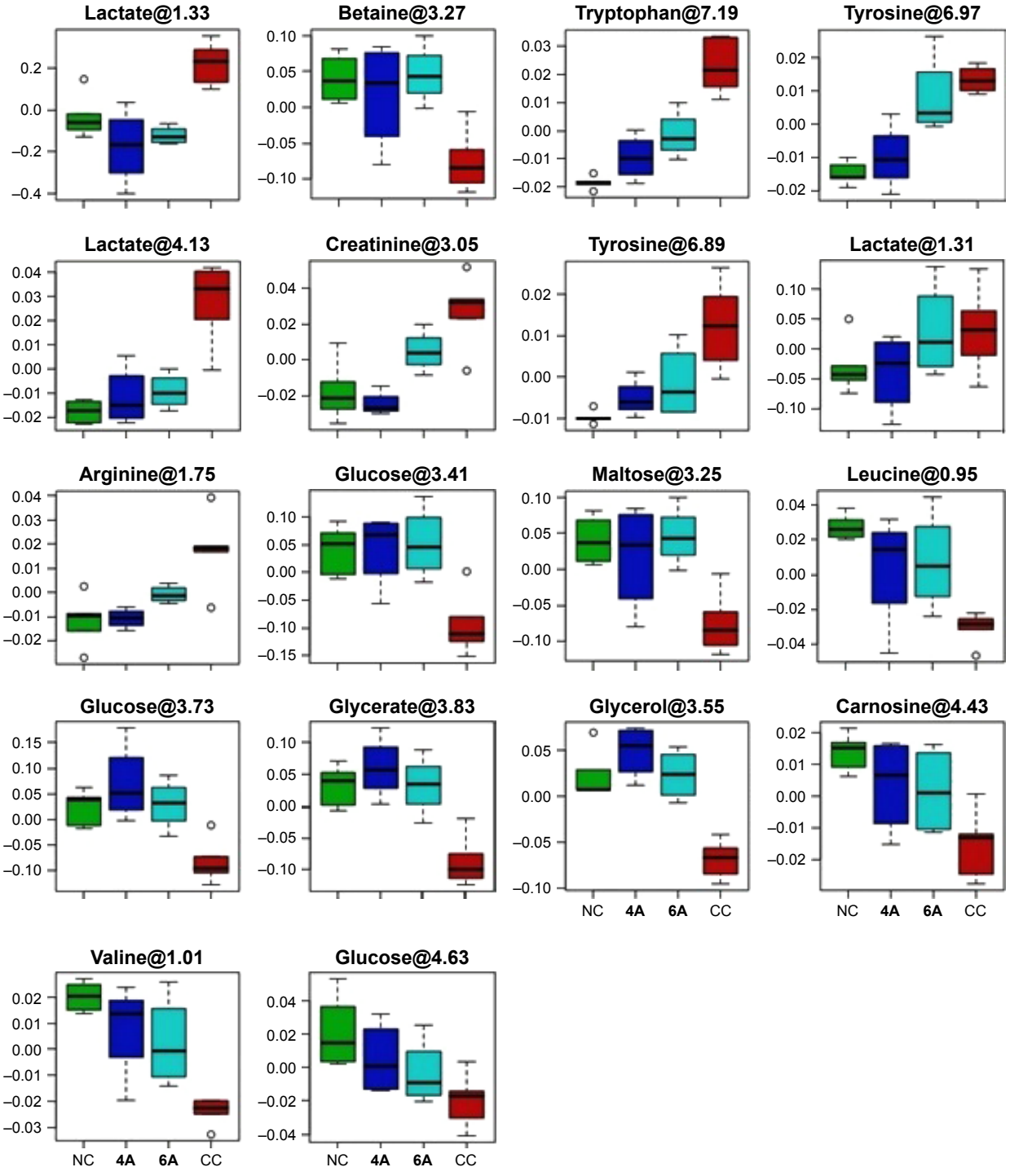

Figure 8 Metabolic effects of **4A** and **6A** treatment.

Notes: The box-cum-whisker plots show relative variations in quantitative profiles of serum metabolites relevant in the context of the pathophysiology of hepatocellular carcinoma. The metabolites highlighted in green color are the metabolites whose *p*-value was found not to be significant ($p>0.05$). In the box plots, the boxes denote interquartile ranges, horizontal line inside the box denote the median, and bottom and top boundaries of boxes are 25th and 75th percentiles, respectively. Lower and upper whiskers are 5th and 95th percentiles, respectively. NC, CC = NDEA, PC, **4A**, and **6A** =10 mg/kg. The y-axis denotes normalized intensity (au) for all cases.

Abbreviations: CC, carcinogen control; NC, normal control; NDEA, N-nitrosodiethylamine; PC, positive control.

metabolic perturbations in NDEA-exposed HCC progression. OPLS-DA score plots using MetaboAnalyst[59] were derived from 1D ^{1}H CPMG NMR spectral data of rat serum samples of all groups, and the carcinogen-exposed HCC rat serum samples clearly demonstrated significant metabolic alterations in cancerous conditions. The decreasing level of glucose and increasing level of lactate were observed in carcinogen-exposed rats, which are consistent with earlier findings.[60,61]

These findings were fully supported the Warburg effect and may be linked with higher amount of glucose consumption by cancerous tissues followed by formation of lactic acid as byproduct.[61,62] We found that **4A**, **6A** and 5-FU treatment regularized the imbalance of the abovementioned metabolites. In this way, we noticed significant elevated levels of lipoproteins and lipids in HCC rats compared to normal and these are involved in the transportation of hydrophobic lipid molecules in circulation or ECF. Next, lipids are also used for production of energy, for instance, β-oxidation. Therefore, the elevated level could be due to the consequences of energy requirement for cell membrane synthesis and rapid proliferation.[63] Moreover, betaine and glycerol were downregulated in HCC condition. These metabolites are mainly involved in metabolism of choline. **4A** and **6A** administration returned the concentrations of these altered metabolites to normal level, further providing evidence of anticancer activity of **4A** and **6A**.[64] The depleted levels of leucine are in accordance with the previous report on human HCC.[65] Arginine (semi-essential amino acid in humans) is critical for the human cancer growth. It is also involved in protein synthesis as well as diverse aspects of tumor metabolism including the synthesis of nitric oxide, proline, glutamate, polyamines and nucleotides. Elevated level of arginine was found in carcinogen-exposed rat serum samples as compared to drug-treated rat serum samples.[66] Furthermore, serum creatinine, an important intermediate in energy metabolism, was significantly increased in NDEA-induced HCC rats compared to normal control and might be associated with increase in energy demand due to cancer proliferations. Tyrosine was also upregulated in NDEA-induced HCC rats, which might be due to increased catabolism.[64,67] Administration of chemically synthesized anticancer compounds (**4A** and **6A**) remarkably attenuated all these metabolite markers, exhibiting hepatoprotective action of **4A** and **6A** against NDEA-exposed HCC. Overall, the impact of **4A** and **6A** was more prominent at 10 mg/kg dose, which was comparable to the reference chemotherapeutic agent 5-FU.

Conclusion

The results of the present investigation suggest that previously synthesized **4A** and **6A** exerted a chemopreventive effects against experimentally NDEA-induced in vivo HCC in albino Wistar rats and this effect could be attributed to an increased antioxidant profile, restored liver-specific enzymes and decreased expression of oncogenes. Correlations of inflammatory cytokine levels with biochemical markers of HCC were also observed. Effectual treatment with **4A** and **6A** reflected reduction in the development of carcinogenic hepatic nodules and restored the normal histological architecture of system. **4A** and **6A** alter the inflammatory signature to reduce significantly the overexpression of IL-6 and attenuate carcinogenic condition. Additionally, metabolic profiling established that **4A** and **6A** have the ability to normalize several metabolites that were significantly disturbed in NDEA-exposed rats, supporting the anticancer activities of **4A** and **6A** for preventing the endogenous metabolic disorders associated with NDEA-induced liver carcinogenesis. However, various physiological and morphological changes, oxidative parameters, liver marker enzymes, cytokines and proton-NMR based serum metabolite profiles were assessed to evaluate the antitumor effect of **4A** and **6A** against NDEA-induced HCC. Collectively, our findings reveal that the antitumor effect of compound **4A** is more prominent than **6A**. Finally, this study provides evidences toward the potency of both **4A** and **6A** treatment in the amelioration of NDEA-exposed HCC in albino Wistar rats and suggests that they can be considered for a range of therapeutic interventions of hepatic cancer in future.

Acknowledgments

Dr Sudipta Saha would like to thank the University Grants Commission (UGC), New Delhi, India, for UGC-MRP grant (Project no 42-680/2013[SR]) and Department of Science and Technology (DST), India, for DST-SERB project (Ref No DST/SB/EMEQ-320/2014). The authors would like to express their gratitude to Babasaheb Bhimrao Ambedkar University, Lucknow, India, for providing the support and research facilities. The authors also express their sincere gratitude to Centre of Biomedical Research, Lucknow, India, for providing the NMR facilities.

Author contributions

Study protocol design: Sudipto Saha, Amit K Keshari; pharmacological screening: Amit K Keshari, Ashok K Singh, Pranesh Kumar, Vinit Raj, Amit Rai, Sudipto Saha; NMR-based metabolomics data analysis: Dinesh Kumar, Umesh Kumar, Amit K Keshari; gene expression studies: Sneha Nath, Anand Prakash; pharmacological data analysis and statistics with preparation of tables and figures: Amit K Keshari, Sudipto Saha, Biswanath Maity, Dinesh Kumar, Anand Prakash; wrote the manuscript: Amit K Keshari, Sudipto Saha, Biswanath Maity, Dinesh Kumar, Anand Prakash. All authors revised the manuscript for important intellectual content.

Disclosure

The authors report no conflicts of interest in this work.

References

1. Velu P, Vijayalakshmi A, Iyappan P, Indumathi D. Evaluation of antioxidant and stabilizing lipid peroxidation nature of *Solanum xanthocarpum* leaves in experimentally diethylnitrosamine induced hepatocellular carcinogenesis. *Biomed Pharmacother*. 2016;84:430–437.
2. Heindryckx F, Colle I, Van Vlierberghe H. Experimental mouse models for hepatocellular carcinoma research. *Int J Exp Pathol*. 2009;90(4):367–386.
3. Raghunandhakumar S, Paramasivam A, Senthilraja S, et al. Thymoquinone inhibits cell proliferation through regulation of G1/S phase cell cycle transition in N-nitrosodiethylamine-induced experimental rat hepatocellular carcinoma. *Toxicol Lett*. 2013;223(1):60–72.
4. Kumar M, Verma V, Nagpal R, et al. Effect of probiotic fermented milk and chlorophyllin on gene expressions and genotoxicity during AFB1-induced hepatocellular carcinoma. *Gene*. 2011;490(1–2):54–59.
5. Kawajiri K, Fujii-Kuriyama Y. P450 and human cancer. *Jpn J Cancer Res*. 1991;82(12):1325–1335.
6. Gupta P, Bansal MP, Koul A. Evaluating the effect of lycopene from *Lycopersicum esculentum* on apoptosis during NDEA induced hepatocarcinogenesis. *Biochem Biophys Res Commun*. 2013;434(3):479–485.
7. World Health Organization. Cancer fact sheet, February 2017. Available from: http://www.who.int/mediacentre/factsheets/fs297/en/. Accessed May 19, 2017.
8. Hashim D, Boffetta P, La Vecchia C, et al. The global decrease in cancer mortality: trends and disparities. *Ann Oncol*. 2016;27(5):926–933.
9. Chacko S, Samanta S. A novel approach towards design, synthesis and evaluation of some Schiff base analogues of 2-aminopyridine and 2-aminobezothiazole against hepatocellular carcinoma. *Biomed Pharmacother*. 2017;89:162–176.
10. Kew MC. Hepatocellular carcinoma: epidemiology and risk factors. *J Hepatocell Carcinoma*. 2014;1:115–125.
11. Marin JJG, Castaño B, Martinez-Becerra P, Rosales R, Monte MJ. Chemotherapy in the treatment of primary liver tumours. *Cancer Ther*. 2008;6(2):711–728.
12. Park SH, Lee Y, Han SH, et al. Systemic chemotherapy with doxorubicin, cisplatin and capecitabine for metastatic hepatocellular carcinoma. *BMC Cancer*. 2006;6:3.
13. Okada S. Cancer chemoprevention as adjuvant therapy for hepatocellular carcinoma. *Jpn J Clin Oncol*. 2001;31(8):357–358.
14. Qin X, Lv Y, Liu P, et al. Novel morpholin-3-one fused quinazoline derivatives as EGFR tyrosine kinase inhibitors. *Bioorg Med Chem Lett*. 2016;26(6):1571–1575.
15. Vodnala S, Bhavani AK, Kamutam R, Naidu VG, Promila, Prabhakar Ch. DABCO-catalyzed one-pot three component synthesis of dihydropyrano[3,2-c]chromene substituted quinazolines and their evaluation towards anticancer activity. *Bioorg Med Chem Lett*. 2016;26(16):3973–3977.
16. Rahman MU, Jeyabalan G, Saraswat P, Parveen G, Khan S, Yar MS. Quinazolines and anticancer activity: a current perspectives. *Synth Commun*. 2017;47(5):379–408.
17. Monchaud D, Allain C, Teulade-Fichou MP. Development of a fluorescent intercalator displacement assay (G4-FID) for establishing quadruplex-DNA affinity and selectivity of putative ligands. *Bioorg Med Chem Lett*. 2016;16(18):4842–4845.
18. Chen X, Du Y, Sun H, Wang F, Kong L, Sun M. Synthesis and biological evaluation of novel tricyclic oxazine and oxazepine fused quinazolines. Part 1: erlotinib analogs. *Bioorg Med Chem Lett*. 2014;24(3):884–887.
19. Zahedifard M, Faraj FL, Paydar M, et al. Synthesis of apoptotic new quinazolinone-based compound and identification of its underlying mitochondrial signalling pathway in breast cancer cells. *Curr Pharm Des*. 2015;21(23):3417–3426.
20. Chandregowda V, Kush AK, Chandrasekara Reddy G. Synthesis and in vitro antitumor activities of novel 4-anilinoquinazoline derivatives. *Eur J Med Chem*. 2009;44(7):3046–3055.
21. Alagarsamy V, Raja Solomon V, Dhanabal K. Synthesis and pharmacological evaluation of some 3-phenyl-2-substituted-3H-quinazolin-4-one as analgesic, anti-inflammatory agents. *Bioorg Med Chem*. 2007;15(1):235–241.
22. Nandy P, Vishalakshi MT, Bhat AR. Synthesis and antitubercular activity of Mannich bases of 2-methyl-3H-quinazolin-4-ones. *Indian J Heterocycl Chem*. 2006;15(3):293–294.
23. Georgey H, Abdel-Gawad N, Abbas S. Synthesis and anticonvulsant activity of some quinazolin-4-(3H)-one derivatives. *Molecules*. 2008;13(10):2557–2569.
24. Verhaeghe P, Azas N, Gasquet M, et al. Synthesis and antiplasmodial activity of new 4-aryl-2-trichloromethylquinazolines. *Bioorg Med Chem Lett*. 2008;18(1):396–401.
25. Ismail MA, Barker S, Abau-el-Ella DA, Abouzid KA, Toubar RA, Todd MH. Design and synthesis of new tetrazolyl- and carboxybiphenylylmethyl–quinazolin-4-one derivatives as angiotensin II AT1 receptor antagonists. *J Med Chem*. 2006;49(5):1526–1535.
26. Malamas MS, Millen J. Quinazolineacetic acids and related analogues as aldose reductase inhibitors. *J Med Chem*. 1991;34(4):1492–1503.
27. Keshari AK, Singh AK, Raj V, et al. *p*-TSA-promoted syntheses of 5H-benzo[h]thiazolo[2,3-b]quinazoline and indeno[1,2-d]thiazolo[3,2-a]pyrimidine analogs: molecular modeling and in vitro antitumor activity against hepatocellular carcinoma. *Drug Des Devel Ther*. 2017;11:1623–1642.
28. Matsuzaki T, Murase N, Yagihashi A, et al. Liver transplantation for diethylnitrosamine-induced hepatocellular carcinoma in rats. *Transplant Proc*. 1992;24(2):748–751.
29. Shiota G, Harada K, Ishida M, et al. Inhibition of hepatocellular carcinoma by glycyrrhizin in diethylnitrosamine-treated mice. *Carcinogenesis*. 1999;20(1):59–63.
30. Furuta K, Sato S, Miyake T, et al. Anti-tumor effects of cimetidine on hepatocellular carcinomas in diethylnitrosamine-treated rats. *Oncol Rep*. 2008;19(2):361–368.
31. Imamoto R, Okano JI, Sawada S, Fujise Y, Abe R, Murawaki Y. Null anticarcinogenic effect of silymarin on diethylnitrosamine-induced hepatocarcinogenesis in rats. *Exp Ther Med*. 2014;7(1):31–38.
32. Mukherjee D, Ahmad R. Glucose-6-phosphate dehydrogenase activity during N′-nitrosodiethylamine-induced hepatic damage. *Achiev Life Sci*. 2015;9(1):51–56.
33. Lodhi RL, Maity S, Kumar P, Saraf SA, Kaithwas G, Saha S. Evaluation of mechanism of hepatotoxicity of leflunomide using albino Wistar rats. *Afr J Pharm Pharmacol*. 2013;7(24):1625–1631.
34. Saha S, Chan DS, Lee CY, et al. Pyrrolidinediones reduce the toxicity of thiazolidinediones and modify their anti-diabetic and anti-cancer properties. *Eur J Pharmacol*. 2012;697(1–3):13–23.
35. Kushwaha PS, Raj V, Singh AK, et al. Antidiabetic effects of isolated sterols from *Ficus racemosa* leaves. *RSC Adv*. 2015;5(44):35230–35237.
36. Keshari AK, Kumar G, Kushwaha PS, et al. Isolated flavonoids from *Ficus racemosa* stem bark possess antidiabetic, hypolipidemic and protective effects in albino Wistar rats. *J Ethnopharmacol*. 2016;181:252–262.
37. Makos BK, Youson JH. Tissue levels of bilirubin and biliverdin in the sea lamprey, *Petromyzon marinus* L., before and after biliary atresia. *Comp Biochem Physiol A Comp Physiol*. 1988;91(4):701–710.
38. Ong MM, Latchoumycandane C, Boelsterli UA. Troglitazone-induced hepatic necrosis in an animal model of silent genetic mitochondrial abnormalities. *Toxicol Sci*. 2007;97(1):205–213.
39. Peinnequin A, Mouret C, Birot O, et al. Rat pro-inflammatory cytokine and cytokine related mRNA quantification by real-time polymerase chain reaction using SYBR green. *BMC Immunol*. 2004;5:3.

40. Schaefer N, Tahara K, von Websky M, et al. Role of resident macrophages in the immunologic response and smooth muscle dysfunction during acute allograft rejection after intestinal transplantation. *Transpl Int*. 2008;21(8):778–791.
41. Wishart DS, Jewison T, Guo AC, et al. HMDB 3.0 – The human Metabolome database in 2013. *Nucleic Acids Res*. 2013;41(Database issue): D801–D807.
42. Nicholson JK, Foxall PJ, Spraul M, Farrant RD, Lindon JC. 750 MHz ^{1}H and ^{1}H-^{13}C NMR spectroscopy of human blood plasma. *Anal Chem*. 1995;67(5):793–811.
43. Guleria A, Bajpai NK, Rawat A, Khetrapal CL, Prasad N, Kumar D. Metabolite characterisation in peritoneal dialysis effluent using high resolution (1)H and (1)H-(13) C NMR spectroscopy. *Magn Reson Chem*. 2014;52(9):475–479.
44. Shahani S. Evaluation of hepatoprotective efficacy of APCL-A polyherbal formulation in vivo in rats. *Ind Drug*. 1999;36:628–631.
45. Rossi L, Zoratto F, Papa A, et al. Current approach in the treatment of hepatocellular carcinoma. *World J Gastrointest Oncol*. 2010; 2(9):348–359.
46. Ueda H, Fukuchi H, Tanaka C. Toxicity and efficacy of hepatic arterial infusion chemotherapy for advanced hepatocellular carcinoma. *Oncol Lett*. 2012;3(2):259–263.
47. Newman DJ. Natural products as leads to potential drugs: an old process or the new hope for drug discovery? *J Med Chem*. 2008; 51(9):2589–2599.
48. Saha S. *Hepatotoxicity of Thiazolidinedione Antidiabetic Drugs: a Structural Toxicity Relationship Study*. *Ph.D*. [Thesis]. National University of Singapore; 2010.
49. Kweon S, Park KA, Choi H. Chemopreventive effect of garlic powder diet in diethylnitrosamine-induced rat hepatocarcinogenesis. *Life Sci*. 2003;73(19):2515–2526.
50. Pradeep K, Mohan CV, Gobianand K, Karthikeyan S. Silymarin modulates the oxidant-antioxidant imbalance during diethylnitrosamine induced oxidative stress in rats. *Eur J Pharmacol*. 2007; 560(2–3):110–116.
51. Kowsalya R, Kaliaperumal J, Vaishnavi M, Namasivayam E. Anticancer activity of *Cynodon dactylon* L. root extract against diethyl nitrosamine induced hepatic carcinoma. *South Asian J Cancer*. 2015;4(2):83–87.
52. Wu H, Li N, Jin R, et al. Cytokine levels contribute to the pathogenesis of minimal hepatic encephalopathy in patients with hepatocellular carcinoma via STAT3 activation. *Sci Rep*. 2016;6:18528.
53. Montoliu C, Piedrafita B, Serra MA, et al. IL-6 and IL-18 in blood may discriminate cirrhotic patients with and without minimal hepatic encephalopathy. *J Clin Gastroenterol*. 2009;43(3):272–279.
54. Onal IK, Akdogan M, Oztas E, et al. Does interleukin-18 play a role in the pathogenesis of hepatic encephalopathy? *Hepatogastroenterology*. 2011;58(106):497–502.
55. Luo M, Li L, Yang EN, Dai CY, Liang SR, Cao WK. Correlation between interleukin-6 and ammonia in patients with overt hepatic encephalopathy due to cirrhosis. *Clin Res Hepatol Gastroenterol*. 2013;37(4):384–390.
56. Chang Q, Daly L, Bromberg J. The IL-6 feed-forward loop: a driver of tumorigenesis. *Semin Immunol*. 2014;26(1):48–53.
57. Germain D, Frank DA. Targeting the cytoplasmic and nuclear functions of signal transducers and activators of transcription 3 for cancer therapy. *Clin Cancer Res*. 2007;13(19):5665–5669.
58. Othman MS, Aref AM, Mohamed AA, Ibrahim WA. Serum levels of interleukin-6 and interleukin-10 as biomarkers for hepatocellular carcinoma in Egyptian patients. *ISRN Hepatol*. 2013;2013:412317.
59. Xia J, Sinelnikov IV, Han B, Wishart DS. MetaboAnalyst 3.0 – making metabolomics more meaningful. *Nucleic Acids Res*. 2015;43(W1): W251–W257.
60. Sahdev AK, Raj V, Singh AK, et al. Ameliorative effects of pyrazinoic acid against oxidative and metabolic stress manifested in rats with dimethylhydrazine induced colonic carcinoma. *Cancer Biol Ther*. 2017;18(5):304–313.
61. Wang H, Wang L, Zhang H, et al. ^{1}H NMR-based metabolic profiling of human rectal cancer tissue. *Mol Cancer*. 2013;12(1):121.
62. Gribbestad IS, Petersen SB, Fjøsne HE, Kvinnsland S, Krane J. 1H NMR spectroscopic characterization of perchloric acid extracts from breast carcinomas and non-involved breast tissue. *NMR Biomed*. 1994;7(4):181–194.
63. Liu Y, Hong Z, Tan G, et al. NMR and LC/MS-based global metabolomics to identify serum biomarkers differentiating hepatocellular carcinoma from liver cirrhosis. *Int J Cancer*. 2014;135(3): 658–668.
64. Huang Q, Tan Y, Yin P, et al. Metabolic characterization of hepatocellular carcinoma using nontargeted tissue metabolomics. *Cancer Res*. 2013;73(16):4992–5002.
65. Gao H, Lu Q, Liu X, et al. Application of 1H NMR-based metabonomics in the study of metabolic profiling of human hepatocellular carcinoma and liver cirrhosis. *Cancer Sci*. 2009;100(4):782–785.
66. Delage B, Fennell DA, Nicholson L, et al. Arginine deprivation and argininosuccinate synthetase expression in the treatment of cancer. *Int J Cancer*. 2010;126(12):2762–2772.
67. Fages A, Duarte-Salles T, Stepien M, et al. Metabolomic profiles of hepatocellular carcinoma in a European prospective cohort. *BMC Med*. 2015;13:242.

Supplementary material

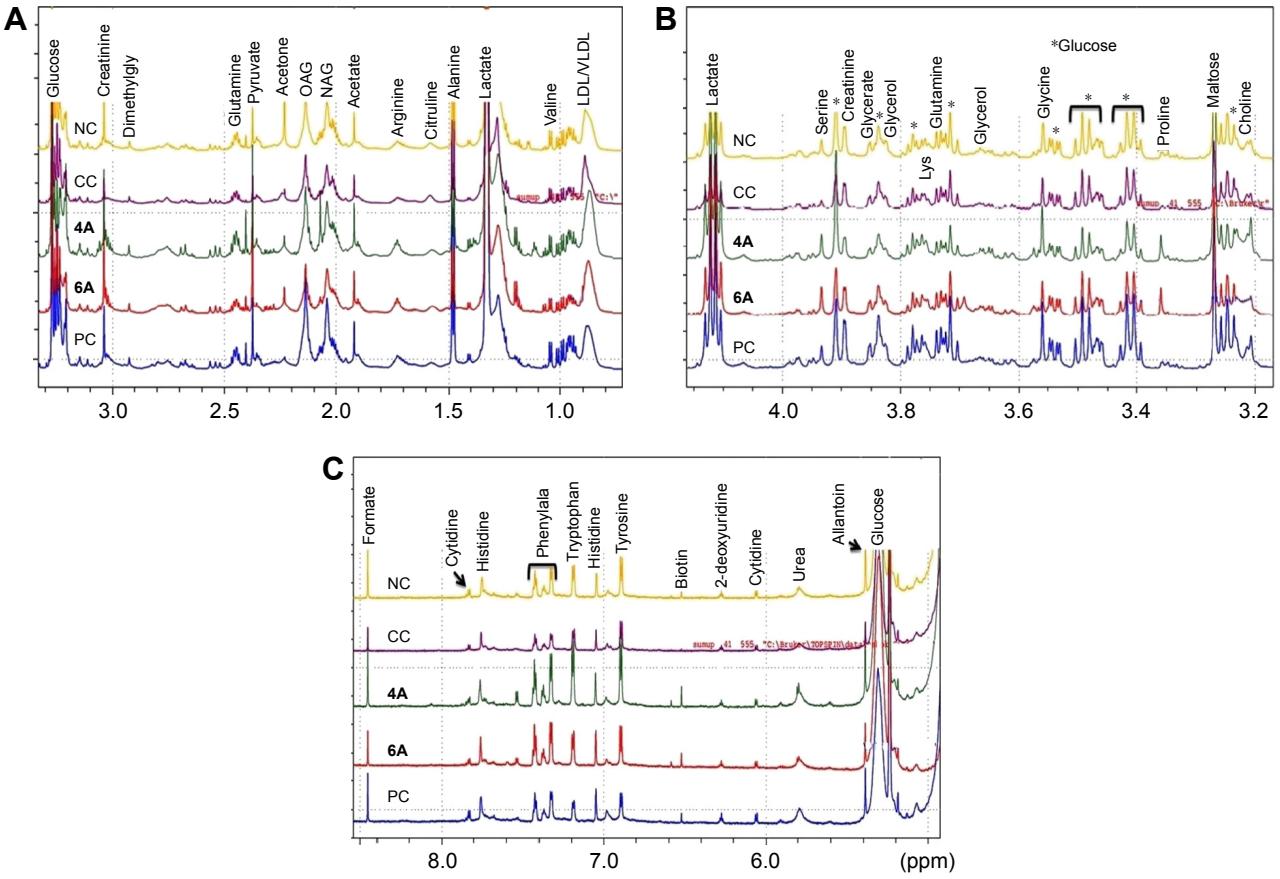

Figure S1 1D ^{1}H CPMG NMR spectra of rat serum obtained from different groups (NC, NDEA [CC], NDEA+5-FU: 10 mg/kg [PC], NDEA+**4A**: 10 mg/kg [**4A**] and NDEA+**6**: 10 mg/kg [**6A**]). The peaks annotated in the figure show the assignments of serum metabolites (**A**) 0–3.0 ppm, (**B**) 3.2–4.0 ppm and (**C**) 5.0–8.0 ppm.
Abbreviations: ^{1}H CPMG NMR, proton Carr–Purcell–Meiboom–Gill nuclear magnetic resonance; CC, carcinogen control; LDL/VLDL, low/very-low density lipoprotein; NAG, N-acetyl glycoprotein; NC, normal control; NDEA, N-nitrosodiethylamine; OAG, O-acetyl glycoprotein; PC, positive control.

Drug Design, Development and Therapy

Dovepress

Publish your work in this journal

Drug Design, Development and Therapy is an international, peer-reviewed open-access journal that spans the spectrum of drug design and development through to clinical applications. Clinical outcomes, patient safety, and programs for the development and effective, safe, and sustained use of medicines are the features of the journal, which has also been accepted for indexing on PubMed Central. The manuscript management system is completely online and includes a very quick and fair peer-review system, which is all easy to use. Visit http://www.dovepress.com/testimonials.php to read real quotes from published authors.

Submit your manuscript here: http://www.dovepress.com/drug-design-development-and-therapy-journal